AD-A074 957 RENSSELAER POLYTECHNIC INST TROY N Y DEPT OF MECHANI--ETC F/G 20/11
A THEORY OF THERMOVISCOPLASTICITY FOR UNIAXIAL MECHANICAL AND T--ETC(U)
JUL 79 E P CERNOCKY, E KREMPL N00014-76-C-0231
UNCLASSIFIED RPI-CS-79-3 NL

1 OF 1
ADA 074957

END
DATE FILMED
11 -79
DDC

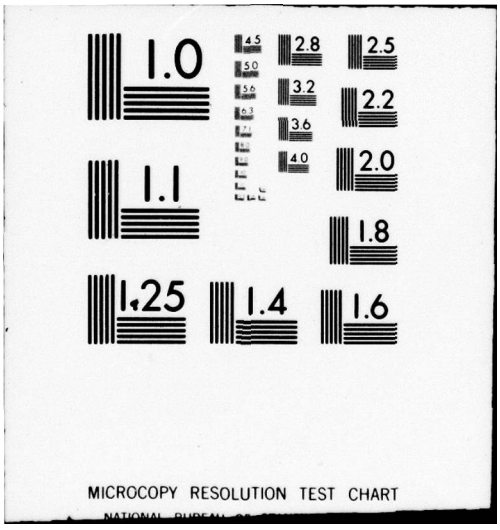
1.0
1.1
1.25
1.4
1.6
1.8
2.0
2.2
2.5
2.8
3.2
3.6
4.0
4.5
5.0
5.6
6.3
7.1
MICROCOPY RESOLUTION TEST CHART

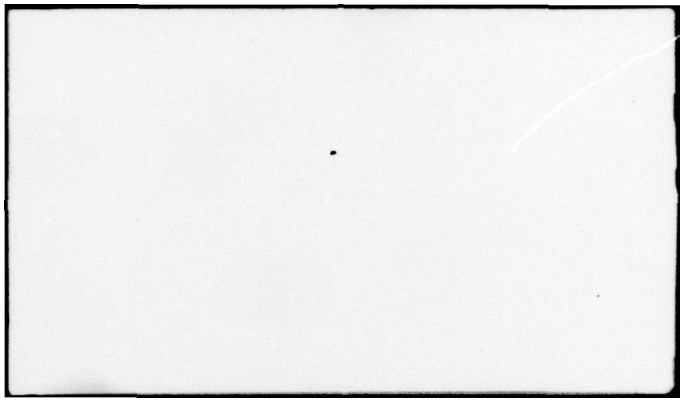

12

A THEORY OF THERMOVISCOPLASTICITY FOR UNIAXIAL MECHANICAL AND THERMAL LOADING

E.P. Cernocky and E. Krempl
Department of Mechanical Engineering,
Aeronautical Engineering & Mechanics
Rensselaer Polytechnic Institute
Troy, New York 12181

Report No. RPI CS 79-3

July 1979

Ser 4473

A THEORY OF THERMOVISCOPLASTICITY FOR UNIAXIAL MECHANICAL AND THERMAL LOADING

E.P. Cernocky and E. Krempl
Department of Mechanical Engineering,
Aeronautical Engineering & Mechanics
Rensselaer Polytechnic Institute
Troy, New York 12181

ABSTRACT

A previously proposed three-dimensional isotropic theory of thermoviscoplasticity based on total infinitesimal strain is specialized to a uniaxial state of stress. This uniaxial theory consists of a first-order differential constitutive equation linear in the mechanical strain rate and the stress rate but nonlinear in the mechanical strain, the temperature, and the stress. This equation is coupled to a constitutive heat equation where the work in a homogeneous, adiabatic cycle which starts and ends at zero stress is completely converted into temperature change. In cyclic loading the mechanical constitutive equation is augmented through a procedure which we call "storage and updating".

The qualitative solution properties of this system of differential equations are investigated. Assuming adiabatic conditions it is shown that near the stress-strain-temperature origin or under large instantaneous changes in the strain (stress) rate, the predicted material behavior is thermoelastic. The solutions for large time under monotonic loadings are given. A set of material constants is assumed; the equations are numerically integrated to simulate homogeneous monotonic loading and cycling and corresponding deformation-induced temperature changes.

Other examples include thermal monotonic and cyclic loading under constraint (thermal fatigue cycling) and mechanical cycling with simultaneous rapid heating.

Introduction

Mechanical deformation is often idealized to occur under isothermal conditions. This idealization is a convenient and a reasonable simplifying assumption under many conditions. In reality mechanical deformation induces temperature changes in materials. Under normal (slow) rates of loading these deformation-induced temperature changes go unnoticed due to the equilibrating effect of heat conduction. However under conditions of rapid monotonic loading or under rapid cyclic loading at sufficiently high stress levels, inelastic self-heating of materials can become important and may result in melting of the material [1]. In particular situations it may become necessary to calculate accurately the temperature changes generated during the course of mechanical deformation; examples are given in [2].

Here we present a coupled theory of thermoviscoplasticity for the uniaxial state of stress and for infinitesimal deformations. To represent the deformation-induced temperature changes which occur during mechanical deformation, we postulate a constitutive heat equation. This equation is coupled to a differential equation governing the mechanical deformation which is called the mechanical constitutive equation. Both equations share a common nonlinear dependence upon the present stress, strain, and temperature, and employ total strain only without any decomposition of strain into separate elastic and inelastic components.

Recent experimental studies [3-6] have indicated that significant rate dependence can be present in the mechanical behavior of metals at elevated and at room temperatures. The mechanical constitutive equation proposed herein is intended to represent both this rate-dependent behavior, and with augmentations the hysteretic behavior observed in metals, including cyclic hardening, cyclic softening, and the Bauschinger effect. Under the

idealization of isothermal deformation the constitutive equation reduces to the previously proposed isothermal mechanical constitutive equation [7].

The purpose of this paper is to examine the behavior predicted by the proposed constitutive equations under homogeneous deformations using a variety of different loading histories including mechanical and thermal cycling. This is accomplished by examining the behavior of the proposed nonlinear coupled differential equations first by analytical means. For hypothetical but realistic material properties the coupled equations are then numerically integrated using the Bulrisch-Stoer Algorithm [22] to illustrate the solution properties in stress-strain and temperature-strain (stress) graphs.

The Constitutive Equations

We designate σ and ϵ as the axial stress and infinitesimal strain, respectively; θ is the absolute temperature and θ_o is the equilibrium or reference temperature. Young's modulus is $E[\theta]$ where throughout this paper brackets denote function dependence upon the indicated argument. The coefficient of thermal expansion is denoted as α and the specific heat of the material is C; here α and C may depend upon absolute temperature or may be taken as constants. A superposed dot denotes time differentiation, while the usual comma-notation is used to represent differentiation with respect to position coordinates. The constant density of the material is denoted as ρ.

We introduce the uniaxial mechanical strain Z as

$$Z = \epsilon - \alpha(\theta - \theta_o) \tag{1}$$

Following [8] we propose our uniaxial mechanical constitutive equation in its simplest form

$$E[\theta]\dot{Z} - \dot{\sigma} = (\sigma - g[Z,\theta])/k[\sigma - g[Z,\theta]] \,. \qquad (2)$$

The function k[ ] is a continuous, positive, even, and decreasing function of its argument. The function $g[Z,\theta]$ represents the equilibrium stress-strain curve of the material at temperature θ. As defined in [7-10] the function g[ ] is odd in Z and for fixed θ and positive Z g[ ] has the appearance of a tensile stress-strain curve; g is initially linear elastic in Z. The second argument of g[ ] represents the temperature dependence of material parameters contained in g[ ] such as $E[\theta]$. We denote the final tangent modulus (in Z) of g[ ] as $E_t[\theta]$, so that for a sufficiently large Z we have $g' \equiv \frac{\partial g[Z,\theta]}{\partial Z} = E_t[\theta]$*. The differential equation (2) is linear in the stress rate, strain rate, and temperature rate, but it is nonlinear in the stress, strain, and temperature through the nonlinear functions k[ ] and g[ ].

Within the context of infinitesimal theory the first law of thermodynamics may be written as

$$\rho\dot{e} = \sigma\dot{\epsilon} - q_{i,i} + \rho R \qquad (3)$$

where e is the internal energy per unit mass, $q_{i,i}$ is the divergence of the heat flux vector, and R is an internal heat supply (which is externally specified and controlled; for example, electric resistance heating). We postulate that the time rate of change of the internal energy is equal to the following exact differential in stress and temperature

---

* Here we assume the stress-strain diagram is ultimately linear in Z. This assumption is convenient but not necessary for the theory.

$$\rho\dot{e} = \rho C[\theta]\dot{\theta} + \frac{d}{dt}\left(\frac{\sigma^2}{2E[\theta]} + \alpha[\theta]\sigma\theta\right) \tag{4}$$

Combining the constitutive assumption (4) with the first law of thermodynamics (3) gives us our equation of heat conduction*

$$(\rho C + \alpha\sigma)\dot{\theta} + q_{i,i} = \sigma\dot{\epsilon} - (\sigma + E\alpha\theta)\frac{\dot{\sigma}}{E} + \rho R \tag{5}$$

where in (5) we surpress writing the temperature dependence of E[ ], C[ ], and α[ ]. To examine heat conduction one must additionally postulate a constitutive choice for the heat flux vector $\underline{q}$. Since we will consider only homogeneous, adiabatic deformations in examining the predictions of this theory, $q_{i,i} = 0$ and a specific choice for the heat flux vector is not necessary.

We note that the constitutive assumption (4) allows us to write in adiabatic deformation without heat supply

$$e = e[\sigma[t], \theta[t], \theta_o]. \tag{6}$$

For adiabatic loading and for zero internal heat supply, Eq. (3) indicates that all of the mechanical work must be converted into change of the internal energy. Experiments indicate that this energy change is manifested through a small percentage of the mechanical work ($\ll 10\%$) being converted into microstructural change and the remaining major portion of the mechanical work being converted into heat [11-14]. For the purposes of this paper we assume that the mechanical work can be completely transformed into temperature change; this assumption corresponds to Eq. (5)

---

* Here and throughout this paper we assume that quantities containing time derivatives of temperature-dependent material parameters can be neglected.

To examine the predictive capability of the theory we first assume the absence of any externally imposed internal heat supply ($R = 0$) in adiabatic deformation. The heat equation (5) may then be rewritten as

$$(\rho C + \alpha\sigma)\,\frac{d\theta}{d\epsilon} = \sigma - (\sigma + E\alpha\theta)\,\frac{d\sigma}{d\epsilon}/E \tag{7}$$

or equivalently using (2) we have

$$\rho C\dot{\theta} = \sigma\,\frac{(\sigma - g[Z,\theta])}{Ek[\ ]} - \alpha\theta\dot{\sigma} \tag{8}$$

or

$$\rho C\dot{\theta} = \frac{(\sigma + E\alpha\theta)\,(\sigma - g[Z,\theta])}{Ek[\ ]} - E\alpha\theta\dot{Z} \tag{9}$$

In all of Eqs. (2) - (9) we may choose either $E = E[\theta]$ or $E =$ constant.

Cyclic Loading

In monotonic tensile or compressive deformations, the sign of the overstress $(\sigma - g)$ predicted by Eqs. (2) and (7) does not change (non-negative in tension, nonpositive in compression). However in cyclic deformations the predicted stress-strain response curve can be forced to cross the equilibrium curve $g[\ ]$ during unloading and reloading*. When such crossing occurs the overstress $(\sigma - g)$ vanishes and subsequently changes sign. At points where the overstress vanishes we (discontinuously) augment the equilibrium function $g[\ ]$ in order to recognize the microstructural changes that have occurred in deforming the material up to this point. Augmentation consists of a process which we call storage and updating.

---

* This cannot occur due to creep or relaxation.

At the occurrence of vanishing overstress, we store the values of the stress, strain, and temperature. We simultaneously may change the value of material constants in the function g[ ] to complete our representation of prior microstructural change. The constant X_f is most suitable for this and in this paper the value of X_f is updated to a new, experimentally determined value*. We then continue the deformation using the augmented equilibrium function in the constitutive equations.

The general idea about augmentation, i.e., the representation of the microstructural changes, was given in [15] and the manner and degree of change of parameters has been presented for the idealization of rate-independent materials in [16]. The procedure used in [16] for the determination of parameter evolution can be extended to this case of rate-dependent materials if the stress-strain curve of [16] is identified as the equilibrium stress-strain curve g[ ] of this report.

Upon initial deformation the material is represented through the g-function which contains material parameters such as X_f [10], which has a constant initial value denoted as $X_f^{(0)}$. We express this state of the material by writing

$$g = g[Z, \theta]\Big|_{X_f^{(0)}} \tag{10}$$

As the material is cycled the overstress vanishes prior to changing sign. At this instant we denote the values of the stress, strain, temperature, and mechanical strain as $\sigma^{(1)}$, $\epsilon^{(1)}$, $\theta^{(1)}$, and $Z^{(1)}$, respectively, and we store these constants. We simultaneously update the parameter X_f

---

* The parameter X_f here refers to the g-function representation in [10]. If necessary additional material parameters can be updated.

by changing it to a new value $X_f^{(1)*}$, and we obtain our augmented equilibrium function by replacing the representation of Eq. (10) with

$$g = g[Z - Z^{(1)}, \theta]\Big|_{X_f^{(1)}} + \sigma^{(1)} \tag{11}$$

We continue the deformation using (11) until the next occurrence of vanishing overstress, where the process is repeated. Hence at the nth occurrence of vanishing overstress we obtain through the storage and updating procedure

$$g = g[Z - Z^{(n)}, \theta]\Big|_{X_f^{(n)}} + \sigma^{(n)} \tag{12}$$

To represent the case of cyclic hardening the parameter X_f increases while in cyclic softening X_f decreases. In the case of steady-state cyclic response, the storage process continues but the parameter X_f ceases to change and remains at a fixed value.

Through this storage-updating procedure the material "remembers" the values of the stress, strain, and temperature at each occurrence of vanishing overstress. Between occurrences of vanishing overstress the microstructural changes are incorporated into the model through the nonlinear character of g[ ] and of k[ ] and through the storage of the stress, strain, and temperature at all points of vanishing overstress. Although this storage-updating procedure is applied discontinuously, the response predicted by the model remains smooth. This procedure is independent of the particular control used, i.e., whether stress, strain, or temperature is prescribed. The details of the augmentation procedure will be described in a forthcoming paper.

---

* The new value must be known from experiments, see Fig.7 of [16].

Figure 1 shows the hysteresis loop obtained through the numerical solution of the coupled equations of this model using this storage-updating procedure; the input is a 1 Hz strain-controlled sine wave, and the functions and material parameters used appear in Table 1. Figure 2 shows the predicted temperature response corresponding to the adiabatic cycling of Figure 1. Both elastic cooling and inelastic heating occur over each cycle with a resultant net increase of temperature with each cycle. The qualitative features of Figure 2 correspond to experimentally observed metal behavior [14].

Behavior in the Neighborhood of the Stress-Strain-Temperature Origin

To model metal deformation the function $g[Z,\theta]$ should be approximately linear thermoelastic so that

$$g[Z,\theta] \approx E[\theta]Z \quad \text{when } Z \approx 0 \tag{13}$$

and

$$E[\theta] \approx E[\theta_o] \quad \text{when } \theta \approx \theta_o \tag{14}$$

The condition (13) may be achieved through the representation of the function $g[\ ]$ proposed in [10]. When (13) applies the differential equation (2) reduces to

$$\sigma \approx EZ \tag{15}$$

and the initial mechanical behavior is linear thermoelastic.

Similarly the heat equation at $\sigma = 0$ reduces to

$$\frac{d\theta}{d\epsilon} = \frac{-E\alpha\theta}{\rho C - E\alpha^2\theta} \approx \frac{-E\alpha\theta}{\rho C} \tag{16}$$

and the initial temperature response is thermoelastic [in Eq. (16) the term $E\alpha^2\theta$ is negligible relative to ρC]. Equation (16) indicates that the initial temperature response is independent of the value of the strain rate or

stress rate and is cooling in tension and heating in compression. Subsequently thermoinelastic heating follows when the mechanical behavior becomes inelastic.

We note that the above properties apply also in the neighborhood of vanishing overstress.

Limiting Behavior Predicted by the Constitutive Theory

To examine the behavior predicted by this constitutive theory in constant strain rate and constant stress rate deformations at the extremes of loading rates and at large times, we rewrite the differential equation (2) as a nonlinear integral equation, see [8]. Using the methods of [7-9] we perform the limit of the stress response predicted under limitingly fast and slow constant strain rate deformation and obtain

$$\lim_{\dot{\epsilon}\to 0} \sigma = g[Z,\theta] \tag{17}$$

and

$$\lim_{\dot{\epsilon}\to \infty} \frac{d\sigma}{d\epsilon} = E[\theta] \frac{dZ}{d\epsilon} \tag{18}$$

Corresponding to (17) and (18) the heat equation (7) reduces to the respective forms

$$\frac{d\theta}{d\epsilon} \approx \frac{1}{\rho C}\left(g - \left(\frac{g}{E} + \alpha\theta\right)\frac{dg[Z,\theta]}{d\epsilon}\right) \tag{19}$$

and

$$\frac{d\theta}{d\epsilon} \approx - \frac{E\alpha\theta}{\rho C} \tag{20}$$

where in (19)

$$\frac{d}{d\epsilon} = \frac{\partial}{\partial\epsilon} + \frac{d\theta}{d\epsilon}\frac{\partial}{\partial\theta} . \tag{21}$$

---

* For constant E (18) reduces to $\sigma = EZ$.

Equations (17) and (18) represent the limiting lower and upper bounds, respectively, upon the mechanical response obtained in constant strain-rate deformation; the same limits are obtained for constant stress-rate loading [7,8]. It is because of the limit (17) that we identify the function $g[Z,\theta]$ as the equilibrium response of the material. From the heat equation in the case of infinitely-slow loading we observe that the temperature response is initially thermoelastic but subsequently is thermoinelastic. When the equilibrium response $g[\ ]$ ceases to be elastic in Z, Eq.(19) predicts inelastic self-heating in the material. The rate of temperature change in this inelastic heating is less than that which occurs at nontrivial strain (stress) rates. In the case of infinitely fast loading, the mechanical behavior is thermoelastic, and the corresponding heat equation predicts only thermoelastic behavior - tensile cooling and compressive heating.

In a constant strain rate deformation we take the limit $t \to \infty$ to determine the limiting or steady-state value of the overstress $(\sigma - g)$ and we denote this limit as

$$\{\sigma - g\} = \lim_{t\to\infty} (\sigma - g) \tag{22}$$

Following [7-9] we use the integral representation of the mechanical constitutive equation to determine this limit and we obtain

$$\{\sigma - g\} = (E - E_t)\left(1 - \alpha \frac{d\theta}{d\epsilon}\right)\dot{\epsilon} k[\{\sigma - g\}] \tag{23}$$

Equation (23) is a transcendental equation in $\{\sigma - g\}$ which indicates that the steady-state overstress depends <u>nonlinearly</u> upon the applied strain rate. Alternatively in constant stress rate deformation the differential equation (2) is substituted into the integrand of the integral equation following [8] to obtain the limiting overstress in constant stress rate deformation

$$\{\sigma - g\} = (E - E_t)k[\{\sigma - g\}]\dot{\sigma}/E_t \,. \tag{24}$$

The equivalence of the limits (23) and (24) is established through execution of the time limit of the time derivative of the integral representation which furnishes

$$\lim_{t\to\infty} \frac{d\sigma}{d\epsilon} = E_t\left(1 - \alpha \frac{d\theta}{d\epsilon}\right) \tag{25}$$

in constant strain rate or constant stress rate deformation.

The limits (23) - (25) are rapidly attained asymptotic limits of the response predicted by the constitutive theory. Although we let $t \to \infty$ to obtain the limits, the mechanical response rapidly locks-into the steady-state response corresponding to these limits at very small strains, as shown in Figs.3 and 5 and the examples in [7-9].

Numerical studies of this constitutive theory in simulated deformations indicate that the term $\alpha \frac{d\theta}{d\epsilon}$ appearing in (23) is negligible.

Both (23) and (24) indicate that the difference between steady-state flow stress and steady-state equilibrium response depends nonlinearly upon the applied strain rate or stress rate. Because of this fact, in deformations in which the strain (stress) rate is increased by many orders of magnitude as in Figs.3 and 5, the difference between stress response and equilibrium response in steady-state behavior may <u>not</u> increase by several orders of magnitude; a small increase in this steady-state spacing can be modeled if an appropriate k[ ]-function is used. Consequently increasing the strain (stress) rate can result in a significant but small increase in steady-state flow stress which is controlled by k[ ]. This prediction qualitatively corresponds to the behavior reported in experiments, see [3-5].

Behavior Predicted Under Jumps in Strain Rate or Stress Rate

We examine the behavior predicted under instantaneous jump increases (decreases) in the applied strain (stress) rate. We let $\dot{\epsilon}^-$ denote a tensile strain rate prior to a jump increase or decrease in the strain rate and we let $\dot{\epsilon}^+ = \gamma\dot{\epsilon}^-$ represent the strain rate jump; $\dot{\epsilon}^+$ denotes the strain rate after the jump (we similarly use + and - in the case of the stress-strain and temperature-strain slopes). The factor γ is a large positive constant in the case of a strain rate jump increase and a small positive constant in the case of a strain rate jump decrease in which loading is continued; in the case of a strain rate jump decrease in which reversal (unloading) occurs, γ is negative. From Eq. (2) and the chain rule we have

$$\frac{d\sigma}{d\epsilon} = E\frac{dZ}{d\epsilon} - \frac{\sigma - g[Z,\theta]}{k[\,]\dot{\epsilon}} \quad . \tag{26}$$

Using (26) both before and after the jump in strain rate, we obtain at the point of jump in rate

$$\frac{d\sigma^+}{d\epsilon} = E\frac{dZ^+}{d\epsilon} + \frac{1}{\gamma}\left(\frac{d\sigma^-}{d\epsilon} - E\frac{dZ^-}{d\epsilon}\right) \tag{27}$$

which relates the stress-strain slopes before and after the jump in strain rate. Proceeding similarly with Eq. (7) we obtain

$$\frac{d\theta^+}{d\epsilon} = \frac{1}{\gamma}\frac{d\theta^-}{d\epsilon} - \frac{1}{(\rho C + \alpha\sigma)}\left[\left(\frac{d\sigma^+}{d\epsilon} - \frac{1}{\gamma}\frac{d\sigma^-}{d\epsilon}\right)(\sigma + E\alpha\theta)/E - \sigma\left(1 - \frac{1}{\gamma}\right)\right] . \tag{28}$$

When a large jump increase in the strain rate is imposed $\gamma >> 1$ (typically $\gamma = 10^2$) and the terms containing $\frac{1}{\gamma}$ become negligible in (27) and (28) we obtain

$$\frac{d\sigma^+}{d\epsilon} \approx E\left(1 - \alpha\frac{d\theta^+}{d\epsilon}\right) \approx E \tag{29}$$

and

$$\frac{d\theta^+}{d\epsilon} \approx - \frac{E\alpha\theta}{\rho C} \, . \tag{30}$$

We observe that the mechanical and thermal responses are approximately linear thermoelastic in slope in departing the stress-strain-temperature point corresponding to strain rate jump increase. The mechanical response upon strain rate jump increase is shown in the numerical simulation of Fig.3 while the corresponding temperature response is shown in Fig.4. In Fig.4 we observe thermoelastic cooling immediately following the strain rate increase corresponding to the prediction of (30).

Alternatively if we consider a jump decrease in the strain rate in the region of steady-state stress response $\left(\frac{d\sigma^-}{d\epsilon} \approx E_t << E\right)$ while continuing tensile loading, then $1 >> \gamma > 0$ (typically $\gamma = 10^{-2}$) and the terms with $\frac{1}{\gamma}$ become dominant in (27) and (28). We obtain the prediction of a very large negative slope for the stress response departing the point of strain rate jump decrease $\left(\text{here } \frac{d\sigma^+}{d\epsilon} \approx - E/\gamma\right)$ as shown in Fig.3*. This rapid decay of stress response results in strong heating in the material, as predicted by (28) where $1/\gamma$ dominates, and this heating is illustrated in Fig.4 corresponding to the strain rate jump decrease of Fig.3.

In the cases of jump increase in strain rate and jump decrease in strain rate, the stress response asymptotically merges with the response curve which would have been obtained under initial uniform application of the high (low) constant strain rate deformation; see Fig.3. Thus this theory

---

* We emphasize that this decrease does not represent a reversal, but continued loading.

predicts an absence of "the strain rate history effect" upon stress response; this prediction corresponds to the experimental behavior reported in [3,4]*. However, a "strain rate history effect" upon temperature response under jump in strain rate is evident, Fig.4; experiments have not yet been performed to test for this effect.

To study the behavior under jump in stress rate we use the chain rule to rewrite (2) as

$$\frac{d\epsilon}{d\sigma} = \frac{1}{E} + \alpha \frac{d\theta}{d\sigma} + \frac{\sigma - g}{Ek[\ ]\dot{\sigma}} \tag{31}$$

Following the previous example we let $\dot{\sigma}^+ = \Omega\dot{\sigma}^-$ and we consider jump increase ($\Omega \gg 1$) and jump decrease ($\Omega \ll 1$) in the stress rate in the steady-state region of stress response where $\frac{d\sigma^-}{d\epsilon} \ll E$. Using (31) both before and after the jump in stress rate we obtain at the point of jump in stress rate

$$\frac{d\epsilon^+}{d\sigma} = \frac{1}{E} + \alpha \frac{d\theta^+}{d\sigma} + \frac{1}{\Omega}\left(\frac{d\epsilon^-}{d\sigma} - \frac{1}{E} - \alpha \frac{d\theta^-}{d\sigma}\right) \tag{32}$$

while from the heat equation we obtain

$$(\rho C + \alpha\sigma)\left(\frac{d\theta^+}{d\sigma} - \frac{1}{\Omega}\frac{d\theta^-}{d\sigma}\right) = \sigma\left(\frac{d\epsilon^+}{d\sigma} - \frac{1}{\Omega}\frac{d\epsilon^-}{d\sigma}\right) - \left(1 - \frac{1}{\Omega}\right)\frac{\sigma + E\alpha\theta}{E} . \tag{33}$$

Equations (32) and (33), respectively, relate the strain-stress and the temperature-stress slopes before and after the jump in stress rate. With a sufficiently large jump increase in stress rate the terms involving $\frac{1}{\Omega}$ are negligible, e.g., if $\frac{1}{\Omega}\frac{d\epsilon^-}{d\sigma} \ll \frac{1}{E}$, and we obtain

---

* In the case of a hypothetical material extremely sensitive to temperature changes, a strain rate history effect would be predicted due to different temperatures resulting at the same strains in the different loading histories.

$$\frac{d\varepsilon^+}{d\sigma} \approx \frac{1}{E} + \alpha \frac{d\theta^+}{d\sigma} \approx \frac{1}{E} \tag{34}$$

and using (34) in (33)

$$\frac{d\theta^+}{d\sigma} \approx - \frac{\alpha\theta}{\rho C} . \tag{35}$$

We observe that under a large instantaneous jump increase in stress rate, both the mechanical and thermal response are approximately linear thermoelastic in departing the point of jump in stress rate; this behavior is illustrated in the numerical simulations of Figs.5 and 6.

Alternatively if we consider a jump decrease in stress rate then $\frac{1}{\Omega}$ is very large (typically $\Omega = 10^{-2}$) and from (32) we obtain

$$\frac{d\sigma^+}{d\varepsilon} \approx \Omega \frac{d\sigma^-}{d\varepsilon} . \tag{36}$$

Thus under large jump decrease in stress rate the mechanical response does not have a large negative slope; rather the response departs the point of jump decrease in stress rate with a very shallow stress-strain slope, as shown in Fig.5. Indeed $\frac{d\sigma^+}{d\varepsilon}$ may become nearly zero for very large jump decreases in stress rate (very small positive Ω). This indicates a strong bias in the theory between behavior under strain control with strain rate jump decrease and behavior under stress control with stress rate jump decrease; such a bias has been observed in experimental studies [3,4]. In the case of strain rate and stress rate jump increase the theory does not predict any bias.

From (33) in the case of jump decrease in stress rate we again obtain a prediction of large rapid heating due to the dominance of $\frac{1}{\Omega}$ in (33) and this prediction is illustrated in the numerical simulation of Fig.6 which corresponds to the mechanical behavior of Fig.5.

Thermal Monotonic Loading and Thermal Cycling

The theory is capable of representing loadings in which both the mechanical quantities (stress or strain) and the temperature are controlled. This requires specification of the internal heat supply term R(t) and here we consider large R(t) in order to prescribe large temperature changes. In this case the deformation-induced temperature changes are small and can be neglected. Then R(t) directly determines the temperature changes and we only need to consider Eq. (2).

Simultaneous changes of the mechanical variables and the temperature occur in elevated temperature applications and are used in mechanical testing. A specific example is thermal fatigue testing [17-19]. In such tests heating is accomplished by passing an electric current through the round bar specimen. Cooling is achieved through conduction and convection [17-19], and an axial (and possibly a radial) temperature gradient is introduced in the specimen.

Thermal stresses are set up at any chosen temperature by preventing the axial motion of the specimen using a suitable clamping device. Clamping may be performed at the minimum or maximum temperatures out of the range over which temperature is cycled, and different stress-temperature hysteresis loops develop depending on the temperature at which clamping takes place [17-19]. During thermal cycling hardening and/or softening can occur and can change the hysteresis loop in a manner similar to the changes observed under strain cycling without external heating.

We idealize this test situation by assuming a uniaxial, homogeneous state of stress and adiabatic conditions; the uniform temperature change is prescribed.

In the first example we consider a bar with zero initial stress corresponding to an initial temperature θ_o and constrained to have zero axial elongation ($\varepsilon = 0$). The bar is subjected to adiabatic heating at various constant temperature rates. Figure 7 shows the compressive stress responses predicted at heating rates from 10^{-2} to 10^{+3} degrees K per second. The insert of Fig.7 shows the temperature-dependent elastic modulus $E[\theta]$ used in this simulation. We see in Fig.7 that the stress response is initially linear elastic in the temperature change but subsequently becomes nonlinear and "thermal softening" sets in. A different choice for the temperature dependence of $E[\theta]$ will alter the curvature of the stress-temperature curves and the thermal softening characteristics. If a constant modulus is chosen, the rate sensitivity of the response will be maintained but the curves will have positive slope for all θ and the thermal softening represented in Fig.7 will disappear.

To simulate thermal cycling we heat to either 900°K or 1200°K and then cycle between 900°K and 1200°K at a frequency of 1 Hz*. In one test we hold the total strain constant at the minimum temperature of the cycle (900°K), Fig.8. Alternatively in Fig.9 the test is begun at the maximum cycle temperature of 1200°K. In each of these cases the $E[\theta]$ of Fig.7 and the update parameters of Fig.1 are used.

We see that in each case stress-temperature hysteresis loops develop similar to the ones observed in experiments, see Figs.4 and 5 of [19]. The increase in tensile stress shown in Figs.8 and 9 is higher than the one observed in experiments. This increase depends on the updating of the

---

* This frequency is faster than the one used in experiments.

parameter X_f which has been arbitrarily selected. The rounded tips of the hysteresis loops are due to the imposed sinusoidal temperature variation.

Simultaneous Mechanical and Thermal Loading

In some experiments the uniaxial specimen is subjected to a specified simultaneous mechanical and thermal loading [20,21]. Here we consider the case of a uniaxial deformation field corresponding to a bar which is cycled with 1 Hz strain control (sine wave) while being rapidly internally heated. Here internal heating corresponds to external specification of the internal heat supply R(t) so that a temperature rate $\dot{\theta} = 300^{\circ}K/sec$ is maintained throughout the strain cycling which starts at an initial temperature of $\theta_o = 300^{\circ}K$. Figure 10 shows the corresponding stress-strain response throughout this combined cycling and heating. At the end of the fourth cycle the temperature of $1500^{\circ}K$ is reached. We see in Fig.10 that this increase in temperature distorts the hysteresis loops and causes cyclic softening although the storage-updating procedure is the same as in Fig.1 where cyclic hardening occurs. The distortion and softening is entirely due to the large specified increase in temperature and the temperature dependence of the g-function through $E[\theta]$. The temperature dependence of E is also responsible for the decrease of the unloading slopes shown in Fig.10.

Discussion

We have examined this theory of thermoviscoplasticity in the case of homogeneous uniaxial deformation. Adiabatic strain cycling and also temperature cycling have been simulated. Also studied were the responses in tensile tests at different strain (stress) rates, the responses to jump increase and jump decrease in the strain (stress) rate, and the mechanical

response to heating at different temperature rates (zero elongation). For consistency only one set of functions k[ ] and g[ ] have been used throughout these simulations; also the same set of material constants, the same value of E when taken to be constant, and the same function E[θ] when taken to be temperature dependent have been used throughout, see Table 1. This procedure facilitates comparison of the figures and assessment of the theory.

In Figs.1 - 5 we see that the temperature changes due to self heating are small at the strain (stress) rates used. If the adiabatic conditions were to be removed these temperature changes could easily be equilibrated through heat conduction.

In the adiabatic cycling the theory presently assumes that the mechanical work (the area of the hysteresis loop measured from zero stress to zero stress) is converted into heat, see Eq.(4). Since cyclic hardening and softening involve small changes in the area of the hysteresis loop, hardening and softening do not have a significant effect on the temperature change generated per cycle. In adiabatic tensile deformation increasing the strain (stress) rate increases the steady-state stress (strain) response; this results in increased self-heating and greater temperature change, as shown in Figs.4,6. In cycling increasing the frequency increases the area of the hysteresis loop moderately which results in a small increase in the temperature change generated per cycle. However, in a fixed period of time a significant temperature increase would result from increasing the frequency because of the increased number of cycles completed in the specified time period.

In the absence of a temperature change the mechanical response predicted by Eq.(2) is symmetric with respect to the origin. In tension the temperature initially decreases but subsequently increases, Figs.4,6. However, in

compression the initial temperature response is immediate and continued heating, see Eq.(16) here and Fig.4 of [8]. Thus the theory predicts that at equal strain (stress) magnitudes the temperature differs slightly in the respective cases of tension and compression. However these differences in the temperature changes are small ($< 1^{\circ}K$) and result in negligible differences between the mechanical responses in tension and compression.

The temperature dependence of material parameters does not significantly influence the response unless large temperature changes are generated. These can occur through very fast adiabatic tensile (compressive) loading, through rapid cycling, or through internal heating (R specified). Temperature dependent material parameters are important in thermal loading because of the large temperature increases that occur. For these conditions significant decreases of the elastic modulus and the yield strength are observed in real materials which must be modelled by the theory.

In our modelling of thermal softening the only temperature-dependent material parameter used is $E[\theta]$ which is shown in the insert of Fig.7. Using this $E[\theta]$ and the g-function proposed in [10], the stress-strain response is predicted to have an initial slope which significantly decreases with increasing initial temperature. Also the corresponding steady-state flow stress is decreased considerably as the initial temperature is increased, see Fig.8 of [8]. The temperature dependence of the modulus is responsible for the thermal softening present in the thermal loading of Fig.7. This also results in the distortion of the strain cycling hysteresis loop of Fig.10. Also the decrease in the flow stress upon reloading in this figure is due to the thermal softening which overcomes the mechanical hardening present in Fig.1.

Figure 8 shows a decrease in the flow stress on the first compressive loading which is much more pronounced than the corresponding case in Fig.9. The curvatures in the tensile and compressive segments of the hysteresis loops of Fig.9 are different. These features result from the temperature dependence of E and the thermal softening*.

We have simulated adiabatic strain cycling (Fig.1), thermal cycling under constraint (Figs.8, 9), and mechanical cycling with simultaneous large internal heating (Fig.10). The same g-function augmentation procedure (storage and updating) and the same successive parameter values (X_f from Table 1) have been used in all cases. Although parameter changes are kept the same to facilitate comparison between the figures, the strain range in Figs.1 and 10 is 1.8% while in Figs.8 and 9 the range of the mechanical strain Z is approximately .4%.

In real materials the amount of hardening will decrease with decreasing strain range; smaller increases in the values of X_f upon updating should be used in Figs.8 and 9 than Figs.1 and 10 to match real material behavior. This would result in a reduction of the amount by which the tensile stress increases with each cycle. Since the points at which overstress vanishes in Figs.8 and 9 correspond to different temperatures from the cases of Figs.1 and 10, a temperature dependence of the parameter X_f in addition to the cycle dependence of X_f would introduce additional flexibility.

---

* As stated earlier the tips of the hysteresis loops are round due to the use of a sine wave as the input; they would be sharp in the case of a saw-tooth input.

The theory presented here is capable of representing both creep and relaxation behavior corresponding to the respective test conditions $\dot{\sigma} = 0$ and $\dot{\epsilon} = 0$. The temperature changes predicted during such deformations are very small and thermomechanical coupling is not important; the properties of the isothermal theory [7,9,23] apply in this case. The theory predicts that relaxation terminates at a nontrivial equilibrium value of stress which is determined by the value of the equilibrium function g[ ], see [7]. Primary and secondary creep can also be modeled [7,23].

Acknowledgement

This work was supported by the National Science Foundation and the Office of Naval Research. The help of A. Meyer who programmed an initial version of this theory is greatly appreciated.

REFERENCES

1. J.F. Tormey and S.C. Britton, Effect of Cyclic Loading on Solid Propellant Grain Structures, AIAA Journal, 1, 1763-1770 (1963).

2. O.W. Dillon, Jr., Some Experiments in Thermoviscoplasticity, in Constitutive Equations in Viscoplasticity, Phenomenological and Physical Aspects, K.C. Valanis, editor, AMD Vol.21, ASME, New York, N.Y., 1976.

3. E. Krempl, An Experimental Study of Room Temperature Rate Sensitivity, Creep, and Relaxation of AISI Type 304 Stainless Steel, J. Mech. Physics of Solids, in press.

4. D. Kujawski and E. Krempl, Rate Sensitivity, Creep and Relaxation of Ti-1AL-2Cb 1Ta Alloy at Room Temperature. An Experimental Study, RPI Report forthcoming.

5. J.A. Bailey and A.R.E. Singer, Effect of Strain Rate and Temperature on the Resistance of Deformation of Aluminum, Two Aluminum Alloys, and Lead, J. Inst. Metals, 92, 404-408 (1964).

6. T. Nicholas, Strain Rate and Strain-Rate History Effects in Several Metals in Torsion, Experimental Mechanics, 11, 370-374 (1971).

7. E.P. Cernocky and E. Krempl, A Nonlinear Uniaxial Integral Constitutive Equation Incorporating Rate Effects, Creep, and Relaxation, RPI Report CS 78-1, to appear in International Journal of Nonlinear Mechanics.

8. E.P. Cernocky and E. Krempl, A Theory of Thermoviscoplasticity Based on Infinitesimal Total Strain, RPI Report CS 79-1 , submitted to International Journal of Solids and Structures.

9. E.P. Cernocky and E. Krempl, A Theory of Viscoplasticity Based on Infinitesimal Total Strain, RPI Report CS 78-3, to appear in Acta Mechanica.

10. E.P. Cernocky and E. Krempl, Construction of Nonlinear Monotonic Functions with Selectable Intervals of Almost Constant or Linear Behavior, Trans. ASME, J. Appl. Mech., 45, 780-784 (1978).

11. G.R. Halford, Stored Energy of Cold Work Changes Induced by Cyclic Deformation, Ph.D. Thesis, University of Illinois, Urbana, Illinois, 1966.

12. F.H. Müller, Thermodynamics of Deformation: Calorimetric Investigations of Deformation Processes, Rheology, 5, edited by F.R. Eirich, Academic Press, 1969.

13. G.I. Taylor and H. Quinney, The Latent Energy Remaining in a Metal after Cold Working, Proc. Roy. Soc., A, 143, 307-326 (1934).

14. S.L. Adams, Ph.D. Thesis, Rensselaer Polytechnic Institute, Forthcoming.

15. E. Krempl, On the Interaction of Rate- and History Dependence in Structural Metals, Acta Mechanica, 22, 53-90 (1975).

16. M.C.M. Liu, E. Krempl and D.C. Nairn, An Exponential Stress-Strain Law for Cyclic Plasticity, Trans. ASME, J. Eng. Materials and Technology, 98, 322 (1976).

17. L.F. Coffin, Jr., A Study of the Effects of Cyclic Thermal Stresses on a Ductile Metal, Trans. ASME, 76, 931-950 (1954).

18. E. Krempl, Ueber die Zeitfestigkeit von Nimonic 80A bei Beanspruchung durch Waermespannungen, Materialpruefung, 5, 274-283 (1963).

19. E. Krempl, Deformation Behavior and Fracture of Nimonic 80A During Thermal Fatigue Cycling Under Constraint, Proceedings of the First International Conference on Fracture, 2, 1637-1662, Sendai, Japan, 1965.

20. C.E. Jaske, Thermal Mechanical Low-Cycle Fatigue of AISI 1020 Steel, in ASTM STP 612, 170-198, American Society for Testing and Materials, 1976.

21. R.H. Stenz, J.T. Berling and J.B. Conway, A Comparison of Combined Temperature and Mechanical Strain-Cycling Data with Isothermal Fatigue Results, Proc. 1st Int. Conf. on Structural Mechanics in Reactor Technology, Paper L5/1, T.A. Jaeger editor, Commission of the European Communities, 1971.

22. R. Bulrisch and J. Stoer, Numerical Treatment of Ordinary Differential Equations by Extrapolation Methods, Num. Math., 8, 1-13 (1966).

23. E. Krempl, Viscoplasticity Based on Total Strain. The Modelling of Creep with Special Considerations of Initial Strain and Aging, to appear in Trans. ASME. J. of Eng. Materials and Technology.

24. M.C.M. Liu and E. Krempl, A Uniaxial Viscoplastic Model Based on Total Strain and Overstress, J. Mech. Physics of Solids, in press.

TABLE 1

MATERIAL FUNCTIONS AND PROPERTIES USED IN THE NUMERICAL EXPERIMENTS

1. General Parameters:

$$\alpha = 14.4 \times 10^{-6} \ (^{\circ}K)^{-1} \qquad \rho C = 3.0 \ MPa/^{\circ}K$$

$$E = 120 \ GPa.$$

In the case of temperature-dependent modulus, $E[\theta]$ is represented by the function shown in Fig.7.

2. The g[ ]-Function; R, E_t, X_f are material constants, see [10]:

$$g[Z,\theta] = E_t Z + \frac{(E[\theta] - E_t)}{2R \tanh[R X_f - 3]} \log_e \left[\frac{\cosh[U]}{\cosh[V]}\right]$$

where

$$U = R(X_f + Z) - 3 \qquad R = R_{min} = 3.6/X_f$$

$$V = R(X_f - Z) - 3 \qquad E_t = 2.5 \ GPa$$

$$X_f = .003.$$

In cycling, Figs.1 and 8 - 10, the parameter X_f is updated at successive occurrences of vanishing overstress. Successive values of X_f are: .00300, .00600, .00625, .00650, .00675, .00700, 0.00725, .00750.

3. The Function k[ ] is Chosen from [24] as:

$$k = B \cdot EXP[21.275 \cdot EXP[-|\sigma - g|/A]]$$

$$B = .2296 \times 10^{-3} \ s$$

$$A = 58.2818 \ MPa$$

FIGURE CAPTIONS

Figure 1 — Completely Reversed Adiabatic Strain Cycling Using a 1 Hz Sine-Wave. Material data from Table 1; E is constant, $\theta_o = 300^\circ K$.

Figure 2 — Deformation-Induced Temperature Change Corresponding to Fig.1.

Figure 3 — Tensile Stress-Strain Diagrams for Piecewise Constant Strain Rate Loading under Adiabatic Conditions. The equilibrium stress-strain curve, the elastic response and the responses to sudden changes in strain rate are also shown. Material data from Table 1; E = const., $\theta_o = 300^\circ K$.

Figure 4 — Adiabatic Temperature Response for the Piecewise Constant Strain Rate Tests 2-7 in Fig.3.

Figure 5 — Tensile Stress-Strain Diagrams for Piecewise Constant Stress Rate Loading under Adiabatic Conditions. The equilibrium stress-strain curve, the elastic response and the responses to sudden changes in stress rate are also shown. Material data from Table 1; E = const, $\theta_o = 300^\circ K$.

Figure 6 — Adiabatic Temperature Response for the Piecewise Constant Stress Rate Tests 2-7 in Fig.5.

Figure 7 — Adiabatic Uniform Heating of a Constrained Bar ($\varepsilon = 0$) at Various Temperature Rates. Material data are given in Table 1. The $E[\theta]$ shown in the insert is used; $\theta_o = 300^\circ K$.

Figure 8 — Adiabatic Thermal Cycling Between 900 and $1200^\circ K$ of a Bar Clamped at $900^\circ K$ (ε = const.) Using a 1 Hz Sine Wave. $E[\theta]$ of Fig.7 is used together with material data from Table 1.

Figure 9 — Same Temperature Cycling, Same Material Data, and Same $E[\theta]$ as in Fig.8 Except for Clamping which Occurs at $1200^\circ K$ (ε = const.)

Figure 10 — Simultaneous 1 Hz Strain Cycling and Uniform Heating at $\dot{\theta} = 300^\circ K\ s^{-1}$ under Adiabatic Conditions. Material data from Table 1 and $E[\theta]$ from Fig.7 are used.

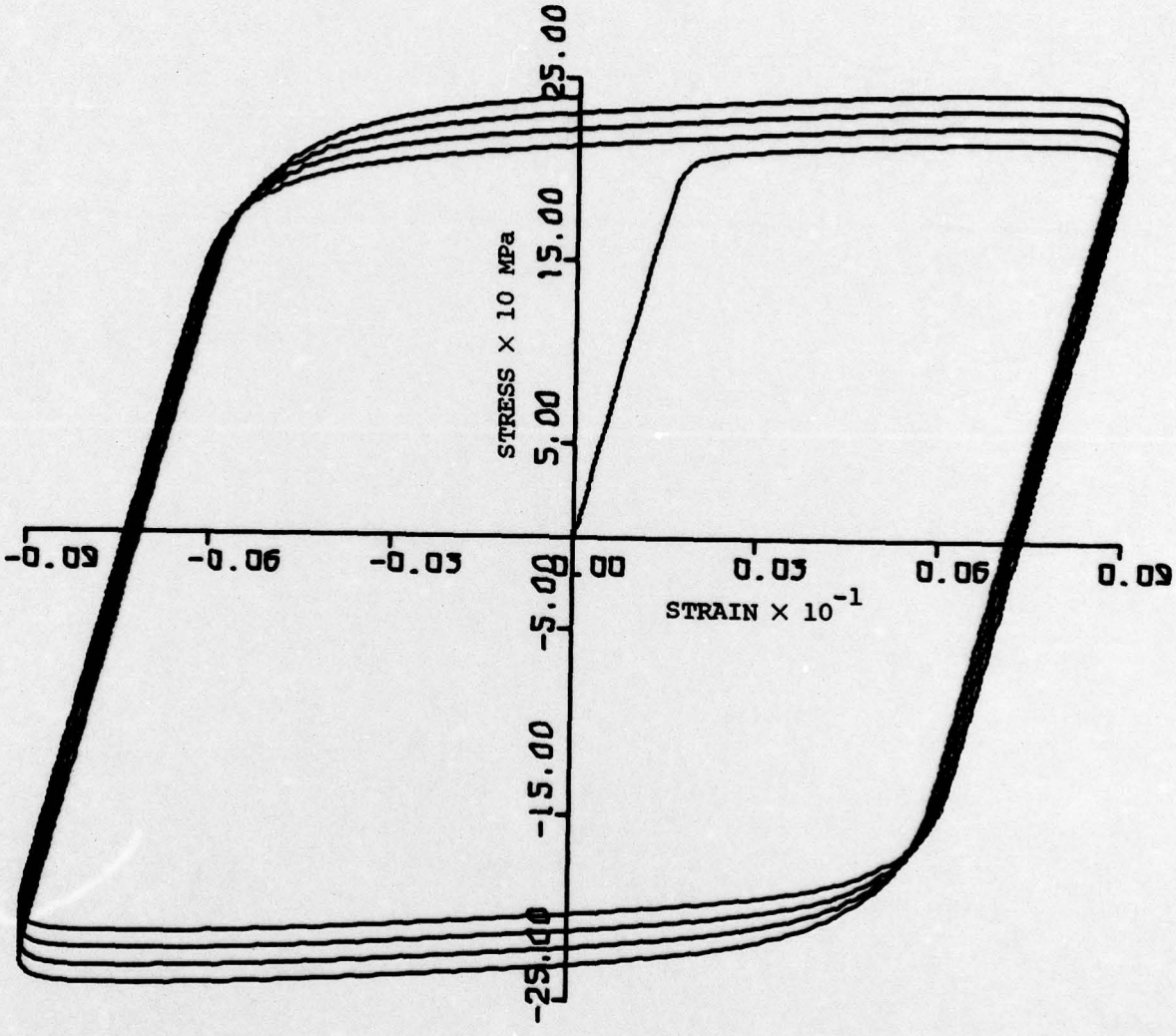
25.00
15.00
5.00
-5.00
-15.00
-25.00
STRESS × 10 MPa
-0.09
-0.06
-0.03
0.00
0.03
0.06
0.09
STRAIN × 10^-1

Figure 1

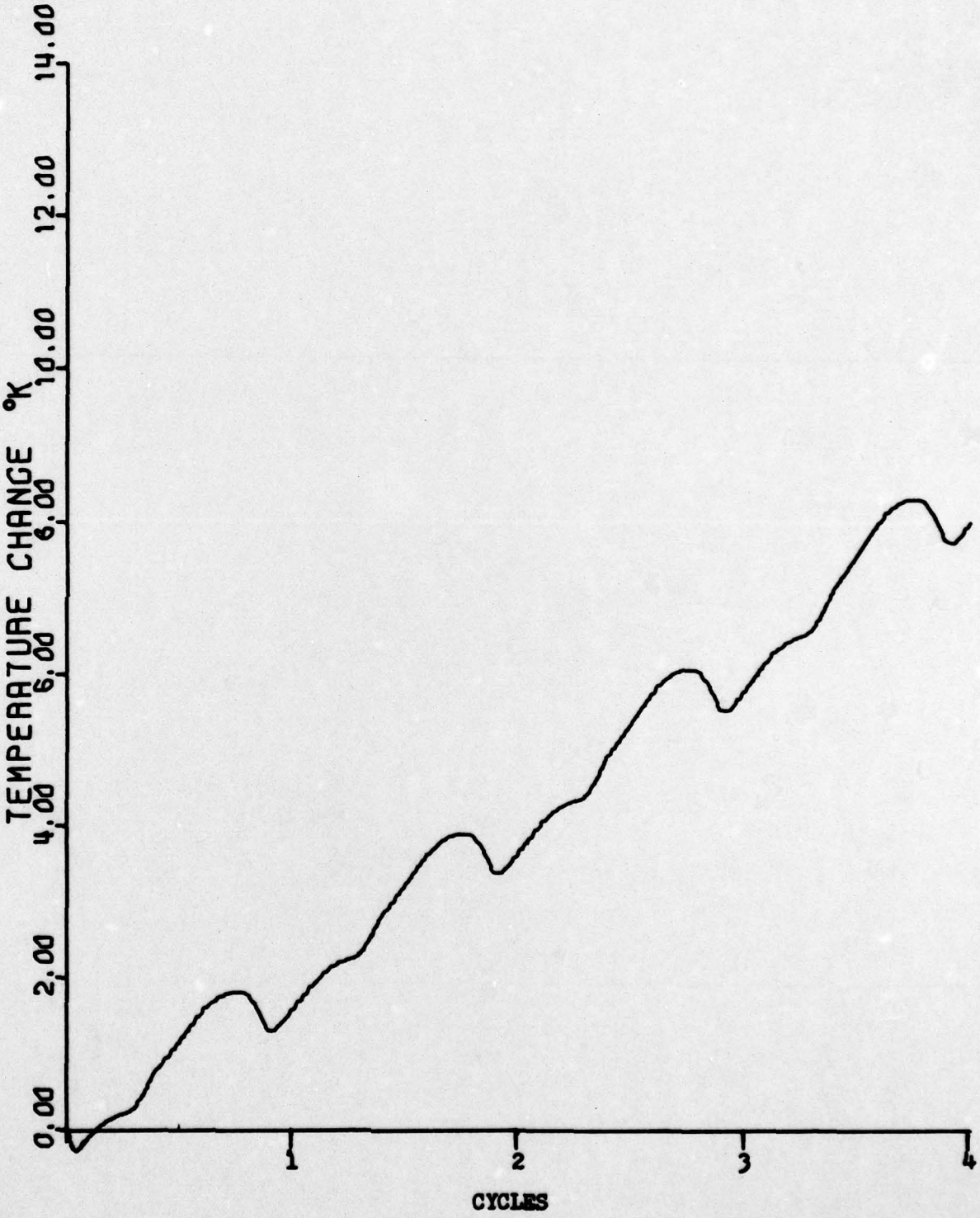
TEMPERATURE CHANGE °K
0.00
2.00
4.00
6.00
6.00
10.00
12.00
14.00
1
2
3
4
CYCLES

Figure 2

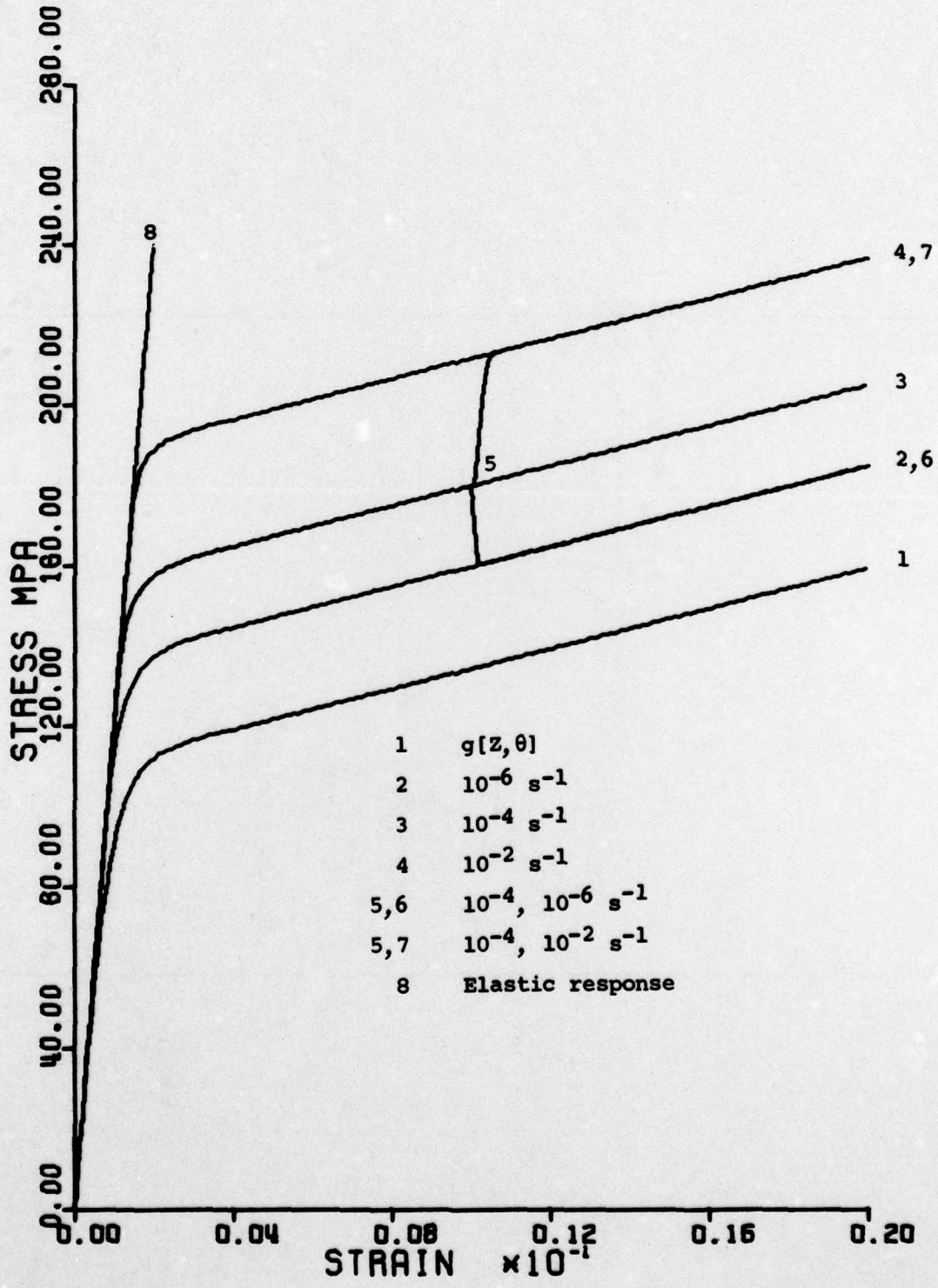
STRESS MPA
0.00
40.00
80.00
120.00
160.00
200.00
240.00
280.00
0.00
0.04
0.08
0.12
0.16
0.20
STRAIN ×10⁻¹
8
4,7
3
5
2,6
1
1 g[Z,θ]
2 10⁻⁶ s⁻¹
3 10⁻⁴ s⁻¹
4 10⁻² s⁻¹
5,6 10⁻⁴, 10⁻⁶ s⁻¹
5,7 10⁻⁴, 10⁻² s⁻¹
8 Elastic response

Figure 3

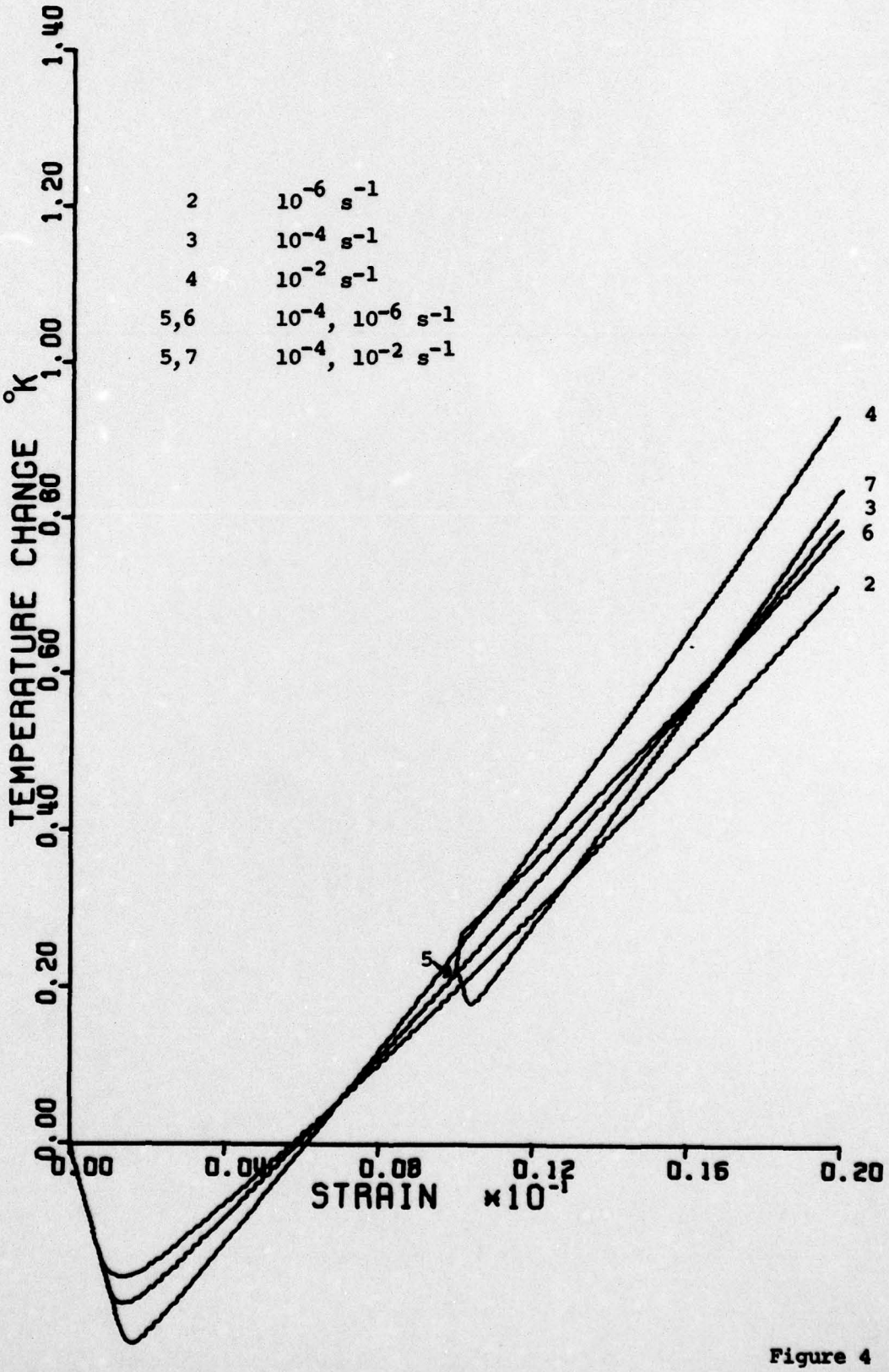
2 10^-6 s^-1
3 10^-4 s^-1
4 10^-2 s^-1
5,6 10^-4, 10^-6 s^-1
5,7 10^-4, 10^-2 s^-1
TEMPERATURE CHANGE °K
0.00
0.20
0.40
0.60
0.80
1.00
1.20
1.40
0.00
0.04
0.08
0.12
0.16
0.20
STRAIN ×10^-1
4
7
3
6
2
5

Figure 4

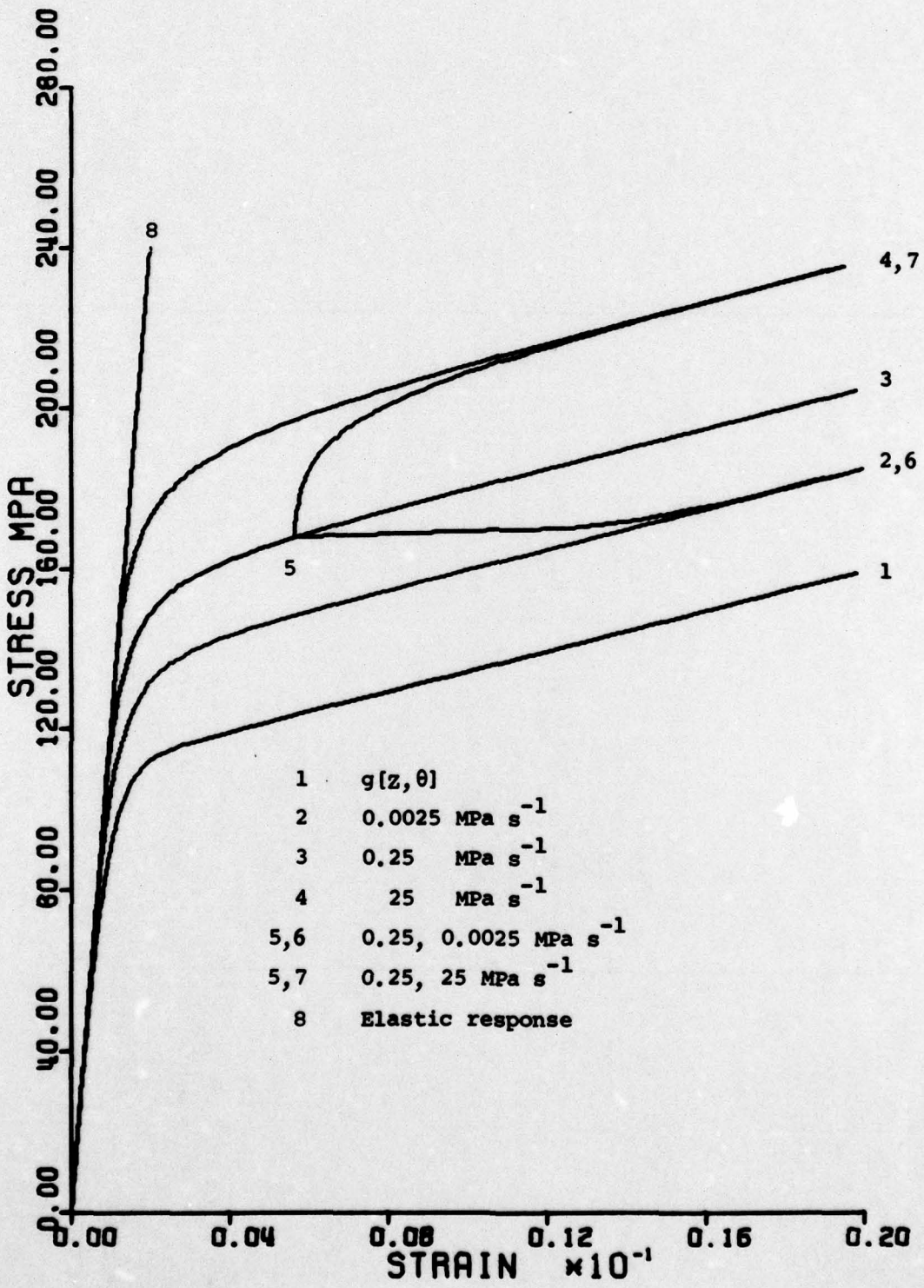
STRESS MPA
0.00
40.00
80.00
120.00
160.00
200.00
240.00
280.00
0.00
0.04
0.08
0.12
0.16
0.20
STRAIN ×10⁻¹
8
4,7
3
2,6
5
1
1 g[z,θ]
2 0.0025 MPa s⁻¹
3 0.25 MPa s⁻¹
4 25 MPa s⁻¹
5,6 0.25, 0.0025 MPa s⁻¹
5,7 0.25, 25 MPa s⁻¹
8 Elastic response

Figure 5

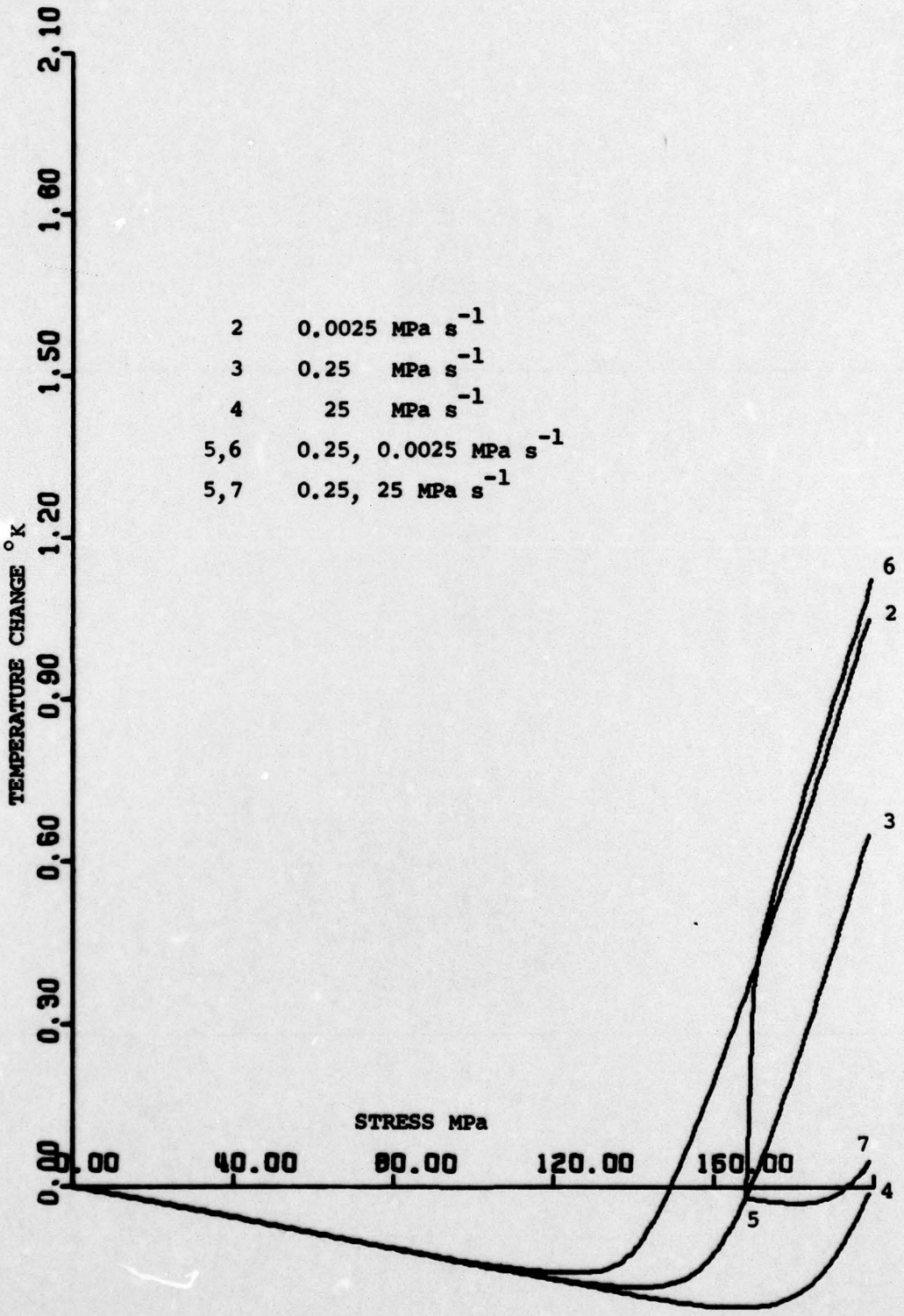
2 0.0025 MPa s^{-1}
3 0.25 MPa s^{-1}
4 25 MPa s^{-1}
5,6 0.25, 0.0025 MPa s^{-1}
5,7 0.25, 25 MPa s^{-1}
TEMPERATURE CHANGE °K
0.00
0.30
0.60
0.90
1.20
1.50
1.80
2.10
STRESS MPa
0.00
40.00
80.00
120.00
160.00
2
3
4
5
6
7

Figure 6

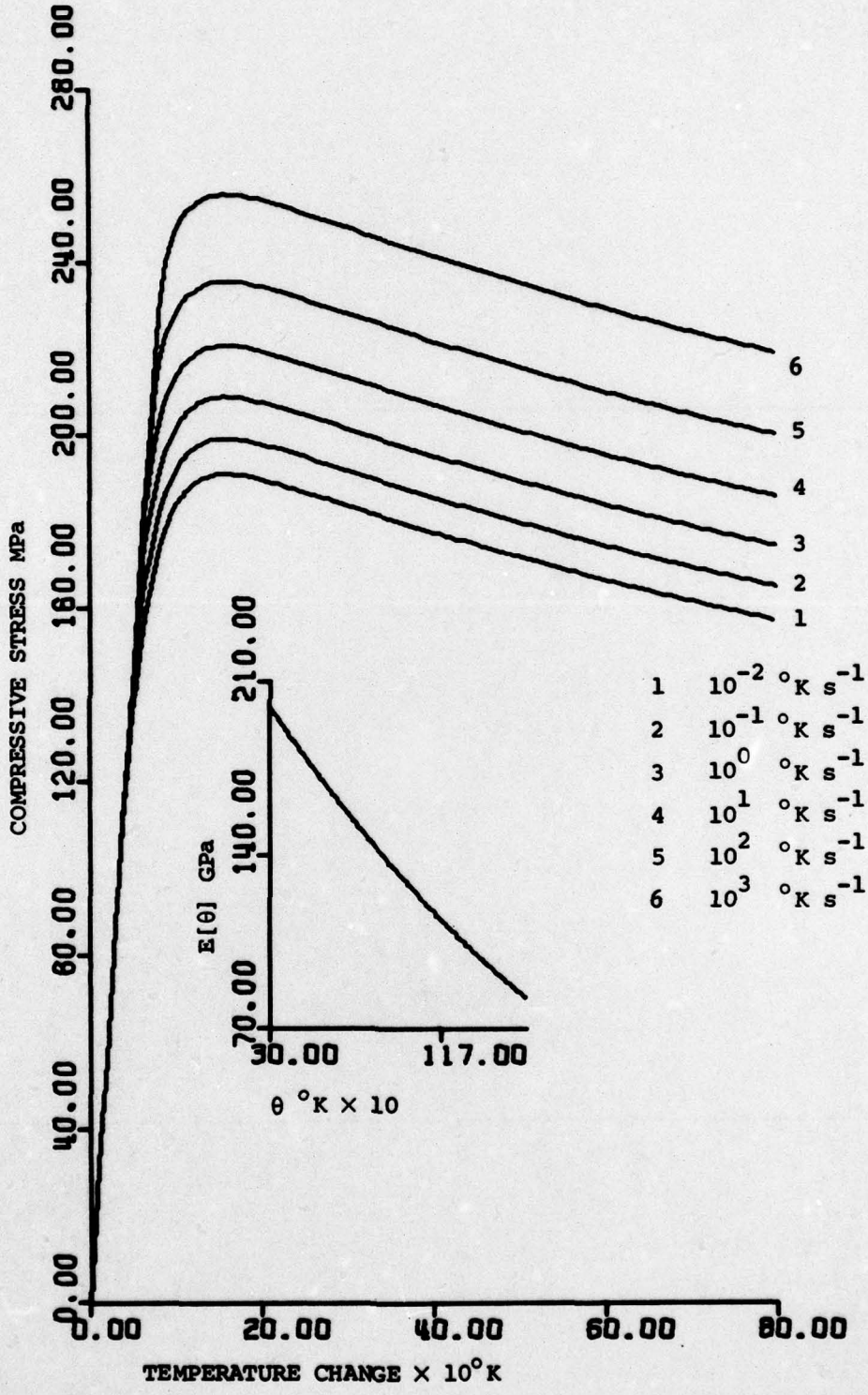
COMPRESSIVE STRESS MPa
0.00
40.00
80.00
120.00
160.00
200.00
240.00
280.00
0.00
20.00
40.00
60.00
80.00
TEMPERATURE CHANGE × 10°K
1
2
3
4
5
6
1 10^-2 °K s^-1
2 10^-1 °K s^-1
3 10^0 °K s^-1
4 10^1 °K s^-1
5 10^2 °K s^-1
6 10^3 °K s^-1
E[θ] GPa
70.00
140.00
210.00
30.00
117.00
θ °K × 10

Figure 7

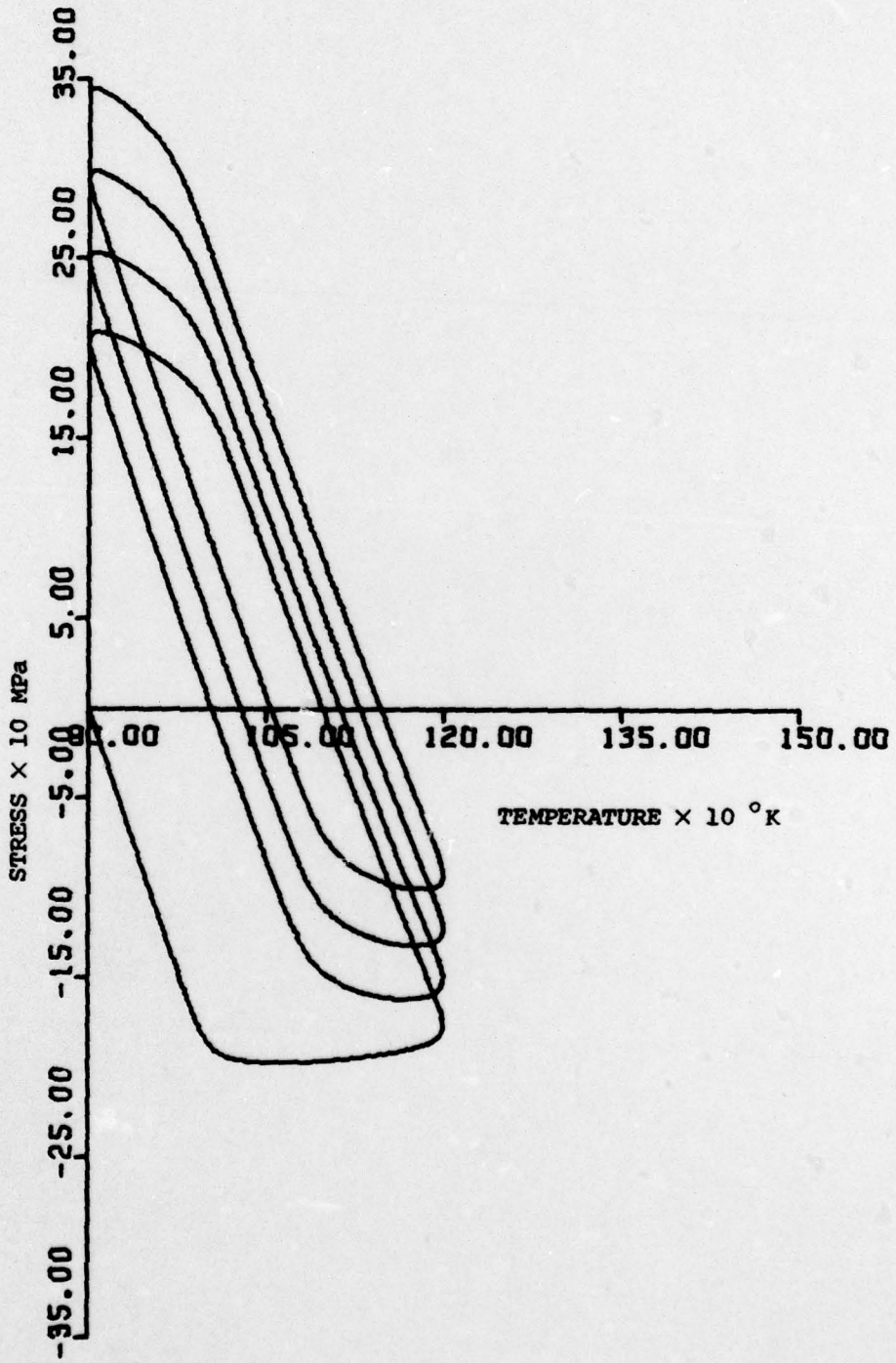
35.00
25.00
15.00
5.00
-5.00
-15.00
-25.00
-35.00
STRESS × 10 MPa
90.00
105.00
120.00
135.00
150.00
TEMPERATURE × 10 °K

Figure 8

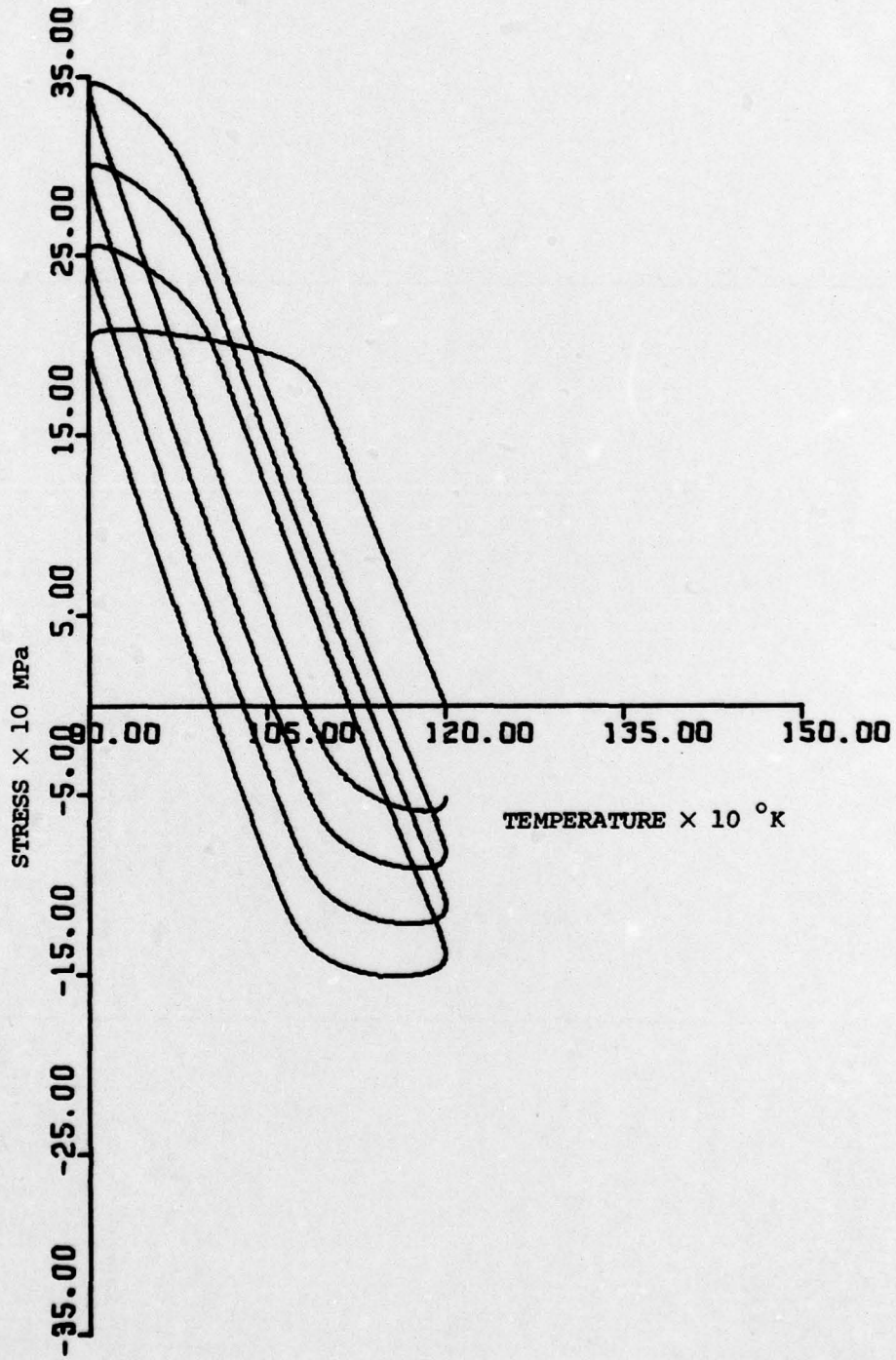
35.00
25.00
15.00
5.00
-5.00
-15.00
-25.00
-35.00
STRESS X 10 MPa
90.00
105.00
120.00
135.00
150.00
TEMPERATURE X 10 °K

Figure 9

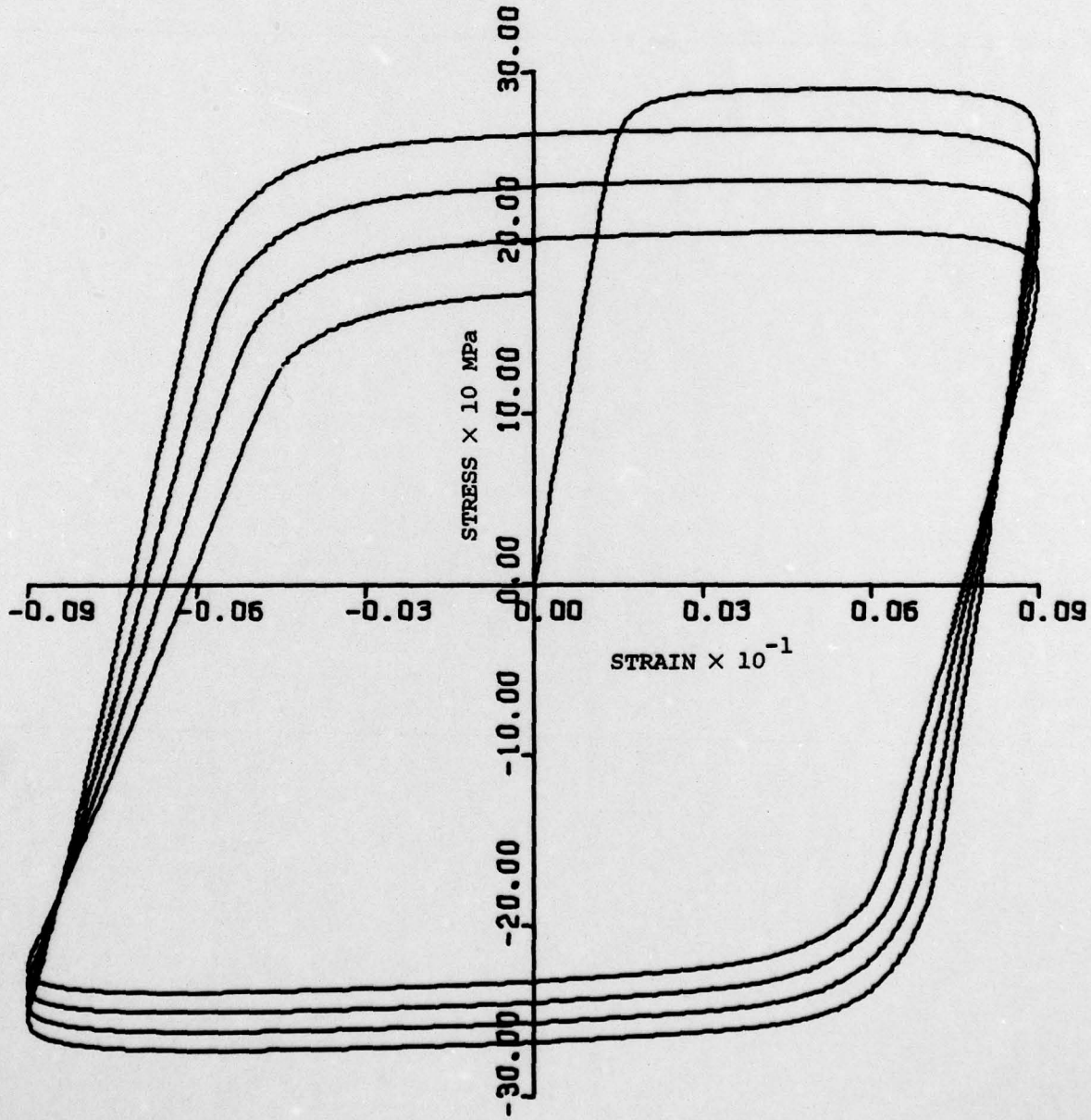
30.00
20.00
10.00
0.00
-10.00
-20.00
-30.00
STRESS × 10 MPa
-0.09
-0.06
-0.03
0.00
0.03
0.06
0.09
STRAIN × 10^-1

Figure 10

Unclassified

SECURITY CLASSIFICATION OF THIS PAGE (When Data Entered)

REPORT DOCUMENTATION PAGE

READ INSTRUCTIONS BEFORE COMPLETING FORM

1. REPORT NUMBER: RPI-CS-79-3	2. GOVT ACCESSION NO.
3. RECIPIENT'S CATALOG NUMBER	
4. TITLE (and Subtitle): A Theory of Thermoviscoplasticity for Uniaxial Mechanical and Thermal Loading.	5. TYPE OF REPORT & PERIOD COVERED: Topical Report
	6. PERFORMING ORG. REPORT NUMBER: RPI CS 79-3
7. AUTHOR(s): E.P. Cernocky and E. Krempl	8. CONTRACT OR GRANT NUMBER(s): N00014-76-C-0231
9. PERFORMING ORGANIZATION NAME AND ADDRESS: Department of Mechanical Engineering, Aeronautical Engineering & Mechanics, Rensselaer Polytechnic Institute, Troy, NY 12181	10. PROGRAM ELEMENT, PROJECT, TASK AREA & WORK UNIT NUMBERS: NR 064-571
11. CONTROLLING OFFICE NAME AND ADDRESS: Dept. of the Navy, Office of Naval Research, Structural Mechanics Program, Arlington, VA 22217	12. REPORT DATE: July 1979
	13. NUMBER OF PAGES: 38
14. MONITORING AGENCY NAME & ADDRESS (if different from Controlling Office): Office of Naval Research - Resident Representative, 715 Broadway - 5th Floor, New York, NY 10003	15. SECURITY CLASS. (of this report): Unclassified
	15a. DECLASSIFICATION/DOWNGRADING SCHEDULE

16. DISTRIBUTION STATEMENT (of this Report)

Approved for public release; distribution unlimited

17. DISTRIBUTION STATEMENT (of the abstract entered in Block 20, if different from Report)

18. SUPPLEMENTARY NOTES

19. KEY WORDS (Continue on reverse side if necessary and identify by block number)

Thermoviscoplasticity, deformation-induced temperature changes, effects of loading rate, cyclic loading, thermal loading, thermal cycling, thermal fatigue, combined thermal-mechanical loading.

20. ABSTRACT (Continue on reverse side if necessary and identify by block number)

A previously proposed three-dimensional isotropic theory of thermoviscoplasticity based on total infinitesimal strain is specialized to a uniaxial state of stress. This uniaxial theory consists of a first-order differential constitutive equation linear in the mechanical strain rate and the stress rate but nonlinear in the mechanical strain, the temperature, and the stress. This equation is coupled to a constitutive heat equation where the work in a homogeneous, adiabatic cycle which starts and ends at zero stress is completely converted into temperature change. In cyclic loading the mechanical (cont'd)

DD FORM 1 JAN 73 1473 EDITION OF 1 NOV 65 IS OBSOLETE S/N 0102-LF-014-6601

Unclassified

SECURITY CLASSIFICATION OF THIS PAGE (When Data Entered)

409 359

constitutive equation is augmented through a procedure which we call "storage and updating".

The qualitative solution properties of this system of differential equations are investigated. Assuming adiabatic conditions it is shown that near the stress-strain-temperature origin or under large instantaneous changes in the strain (stress) rate, the predicted material behavior is thermoelastic. The solutions for large time under monotonic loadings are given. A set of material constants is assumed; the equations are numerically integrated to simulate homogeneous monotonic loading and cycling and corresponding deformation-induced temperature changes.

Other examples include thermal monotonic and cyclic loading under constraint (thermal fatigue cycling) and mechanical cycling with simultaneous rapid heating.